Atmos. Meas. Tech., 4, 97–116, 2011
www.atmos-meas-tech.net/4/97/2011/
doi:10.5194/amt-4-97-2011

Atmospheric Measurement Techniques

Absolute accuracy and sensitivity analysis of OP-FTIR retrievals of CO_2, CH_4 and CO over concentrations representative of "clean air" and "polluted plumes"

T. E. L. Smith[1], **M. J. Wooster**[1,2], **M. Tattaris**[1], **and D. W. T. Griffith**[3]

[1]King's College London, Environmental Monitoring and Modelling Research Group, Department of Geography, Strand, London, WC2R 2LS, UK
[2]NERC National Centre for Earth Observation, UK
[3]University of Wollongong, Centre for Atmospheric Chemistry, Wollongong, NSW 2522, Australia

Received: 15 June 2010 – Published in Atmos. Meas. Tech. Discuss.: 23 August 2010
Revised: 5 January 2011 – Accepted: 6 January 2011 – Published: 26 January 2011

Abstract. When compared to established point-sampling methods, Open-Path Fourier Transform Infrared (OP-FTIR) spectroscopy can provide path-integrated concentrations of multiple gases simultaneously, in situ and near-continuously. The trace gas pathlength amounts can be retrieved from the measured IR spectra using a forward model coupled to a non-linear least squares fitting procedure, without requiring "background" spectral measurements unaffected by the gases of interest. However, few studies have investigated the accuracy of such retrievals for CO_2, CH_4 and CO, particularly across broad concentration ranges covering those characteristic of ambient to highly polluted air (e.g. from biomass burning or industrial plumes). Here we perform such an assessment using data collected by a field-portable FTIR spectrometer. The FTIR was positioned to view a fixed IR source placed at the other end of an IR-transparent cell filled with the gases of interest, whose target concentrations were varied by more than two orders of magnitude. Retrievals made using the model are complicated by absorption line pressure broadening, the effects of temperature on absorption band shape, and by convolution of the gas absorption lines and the instrument line shape (ILS). Despite this, with careful model parameterisation (i.e. the optimum wavenumber range, ILS, and assumed gas temperature and pressure for the retrieval), concentrations for all target gases were able to be retrieved to within 5%. Sensitivity to the aforementioned model inputs was also investigated. CO retrievals were shown to be most sensitive to the ILS (a function of the assumed instrument field-of-view), which is due to the narrow nature of CO absorption lines and their consequent sensitivity to convolution with the ILS. Conversely, CO_2 retrievals were most sensitive to assumed atmospheric parameters, particularly gas temperature. Our findings provide confidence that FTIR-derived trace gas retrievals of CO_2, CH_4 and CO based on modeling can yield results with high accuracies, even over very large (many order of magnitude) concentration ranges that can prove difficult to retrieve via standard classical least squares (CLS) techniques. With the methods employed here, we suggest that errors in the retrieved trace gas concentrations should remain well below 10%, even with the uncertainties in atmospheric pressure and temperature that might arise when studying plumes in more difficult field situations (e.g. at uncertain altitudes or temperatures).

1 Introduction

In many applications, remote sensing of gas species presence and concentrations offer advantages over established point-sampling and/or laboratory analysis methods. Open-path (OP) Fourier Transform Infrared (FTIR) spectroscopy can be used to detect and quantify a wide range of gases simultaneously; can operate in situ, eliminating contamination from tubing or sample handling; can operate continuously, providing real-time data at a relatively high temporal resolution (seconds); and can be used over long path lengths, providing path-integrated gas concentrations less prone to

Correspondence to: T. E. L. Smith
(thomas.smith@kcl.ac.uk)

artefacts induced by point-based sampling and which cannot easily be acquired using alternative approaches.

A variety of analysis techniques are available to retrieve trace gas concentrations from measured single-beam spectra acquired by FTIR instrumentation. These generally involve comparing the measured spectra with reference spectra of the gas of interest under known conditions of temperature, pressure and concentration. Reference spectra may come from laboratory measurements of gases, or may be synthetically generated (e.g. Griffith, 1996) from molecular absorption databases, such as HITRAN (Rothman et al., 2009). One retrieval technique involves converting the measured spectra into absorbance units and fitting the reference spectra using classical least squares (CLS) or partial least squares methods over a spectral window within which the trace gas of interest has significant features (Haaland, 1990). One difficulty with this approach can be the necessity to obtain "background" single beam spectra unaffected by the gases of interest, these being combined with the single-beam observations of interest to derive the values of absorbance (Bacsik et al., 2004). Alternatively, the single-beam reference spectra may be modelled and iteratively fitted to the measured spectra using nonlinear least squares (NLLS) (e.g. Griffith et al., 2003). The accuracy of both methods is generally gauged via a goodness-of-fit measure between the measured and modelled/reference spectra. However, only a few published studies have determined absolute retrieval accuracies via independent accuracy assessments based on experimental methods using cells containing known gas concentrations (see Esler et al., 2000; Horrocks et al., 2001). This is surprising given the sensitivity of retrieval methods to analysis parameters such as spectral window position and extent, gas temperature and pressure, and instrument line shape (Hart et al., 1999; Horrocks et al., 2001). OP-FTIR spectroscopy is being used increasingly as a method for monitoring key carbonaceous greenhouse and tracer species such as CO_2, CH_4 and CO. Given that OP-FTIR spectroscopy of these and other trace gas species is being applied in an ever-increasing range of applications, including volcanology (Horrocks et al., 1999; Oppenheimer et al., 2002); urban and aircraft pollution assessment (Grutter, 2003; Grutter et al., 2003; Hong et al., 2004; Schäfer et al., 1995, 2003) agricultural emission estimation (Childers et al., 2001; Griffith et al., 2002); and biomass burning investigations (Griffith et al., 1991; Yokelson et al., 1997), it is important that the true accuracy of the method is established over the wide range of potential concentrations found in these applications. Here we use an experimentally-based laboratory setup to determine the absolute accuracy of OP-FTIR retrievals of carbon dioxide (CO_2), carbon monoxide (CO) and methane (CH_4) made using the modelling approach across a concentration range encompassing both ambient air and highly polluted plumes (such as those emanating from vegetation fires, vehicle pollution or biogenic sources).

2 Background

In some cases, the accuracy of FTIR retrievals has been inferred via comparisons of the retrieved concentrations to those from more established point-sampling techniques, such as nondispersive infrared (NDIR) spectroscopy for CO_2 and CO (e.g. Gerlach et al., 1998), or gas chromatography (GC) (e.g. Goode et al., 1999) or wet chemistry (e.g. von Bobrutzki et al., 2010) for other gases. For laboratory biomass burning, Goode et al. (1999) compared FTIR concentration retrievals made using synthetic reference spectra and CLS analysis, with those from GC. CO_2 retrievals from FTIR were shown to agree to within 1% of the GC results, although FTIR retrievals of CO and CH_4 were shown to generally underestimate concentrations by ∼6% when compared with GC. Gerlach et al. (1998) compared CO_2/SO_2 ratios derived from FTIR, NDIR and GC, finding general agreement between all three methods. Whilst these results are encouraging in terms of the apparent agreement between FTIR and alternative approaches, they only represent intercomparisons between methods essentially employing rather different sampling strategies.

To achieve a true absolute accuracy assessment for FTIR retrievals, it is necessary to measure the IR spectra of well characterised, laboratory prepared, calibrated gas mixtures and compare the gas concentrations retrieved from these measurements to the known true concentrations. Only a limited number of studies have undertaken such a procedure (e.g. Horrocks et al., 2001; Esler et al., 2000; Lamp et al., 1997). Esler et al. (2000) were primarily interested in determining the precision of FTIR gas analysis of CO_2, CH_4, CO and N_2O, using a sample of clean air (Southern Hemisphere "baseline" air) introduced into a 9.8 m White cell, analysing the measured spectra using a CLS approach and synthetically generated absorbance spectra. For CO_2, the method proved to be highly accurate giving a retrieval accuracy of 0.006% compared to GC analysis of the same sample, and for CH_4, CO and N_2O, 0.03%, 1.0% and 0.1% respectively. These excellent accuracy statistics for ambient air unfortunately were not extended to measurements covering a broader range of concentrations. Optimal retrievals made at higher concentrations (and equivalently longer pathlengths, since the method actually responds to the number of gas molecules present in the optical path) might require use of different parameterisatons of the forward model (for example the spectral window). This maybe due, for example, to absorption saturation or deviations from the standard Beer-Lambert law caused by deviations in absorptivity coefficients at high concentrations due to interactions between molecules in close proximity (Zhu and Griffiths, 1998).

Lamp et al. (1997) generated gas mixtures using mass flow controllers to yield a broad concentration range of CH_4 (8–1900 ppmm) and CO (10–3120 ppmm – parts per million meters) in a 20 m White cell. CLS analysis of the resulting IR absorbance spectra showed a significant nonlinear

relationship between measured and known concentrations. For CH_4, retrieved values were within 5% of the true concentrations below 700 ppmm, but accuracy halved at higher concentrations. Lamp et al. (1997) demonstrated that use of strong absorption regions, such as the CH_4 Q-branch at 3017 cm^{-1}, can lead to reduced accuracy as concentration increases, and a switch to other spectral windows might be more appropriate. CO retrievals were shown to suffer from similar nonlinearities, with concentration underestimated by more than 50% at concentrations higher than 1000 ppmm.

An alternative to CLS-based methods is to use a nonlinear least squares (NLLS) fitting procedure (Marquardt, 1963). This approach can fit single-beam spectra directly and requires no assumption of Beer-Lambert linearity, allowing for the use of both weak and strong absorption regions (Griffith et al., 2003). In a comparison between retrievals made using CLS and NLLS methods, Childers et al. (2002) found that for CO_2, CH_4, NH_3 and N_2O, the CLS method generally underestimated at higher gas concentrations. To demonstrate this effect, Fig. 1 illustrates retrievals made here using the CLS and NLLS approach from spectra of a gas cell containing CO_2 gas of varying concentrations, topped up with nitrogen to maintain ambient pressure (the experimental method is described fully in Sect. 3 of this paper). The underestimation of high CO_2 concentrations when using the CLS method is clearly evident, and is due to the aforementioned nonlinear deviation from the Beer-Lambert law.

For volcanological applications, Horrocks et al. (2001) used a similar experimental setup and spectral modelling approach to that employed here to test the accuracy of OP-FTIR retrievals of SO_2 over a wide range of absorber amounts (125 ppmm–10 500 ppmm). As is the case here, instead of using a White cell to increase pathlength, Horrocks et al. (2001) chose to use higher mixing ratios (ppm) of SO_2, which are equivalent to a longer path according to the Beer-Lambert law:

$$\tau = \alpha\, Lc \tag{1}$$

where optical depth (τ, unitless) is equal to the product of the absorption coefficient of the sample (α, $[\text{ppmm}]^{-1}$), the path length of the sample (L, m) and the mixing ratio of the sample (c, ppm). Optical depth is related to the true transmission (T, unitless) following Eq. (2):

$$T = e^{-\tau} \tag{2}$$

The measured transmittance is the true transmittance convolved with the instrument line shape (ILS). Horrocks et al. (2001) found that increased retrieval accuracies were achieved as concentrations of SO_2 increased, improving from ~5.6% at 125 ppmm to within 1.0% at 10 500 ppmm. This study builds on this work by using a similar approach to establish the OP-FTIR retrieval accuracies for CO_2, CO and CH_4 at mixing ratios ranging from those found in ambient air to those found in polluted cities, biomass burning smoke and volcanic plumes, a much broader range than investigated by Esler et al. (2000). We follow Horrocks et al. (2001) and analyse the collected IR spectra using an iterative NLLS method coupled to a forward modelling approach, specifically the Multi-Atmospheric Layer Transmission (MALT) model described in Griffith (1996) and Griffith et al. (2003). The work of Lamp et al. (1997) showed how Beer-Lambert law divergence can impact retrieval accuracy when investigating high concentration gases using spectral regions containing strong IR absorbance features. Generating retrievals from modelled synthetic spectra fitted to the measured spectra in the way conducted here should avoid these problems and the associated concentration underestimation illustrated in the CLS-derived results displayed Fig. 1.

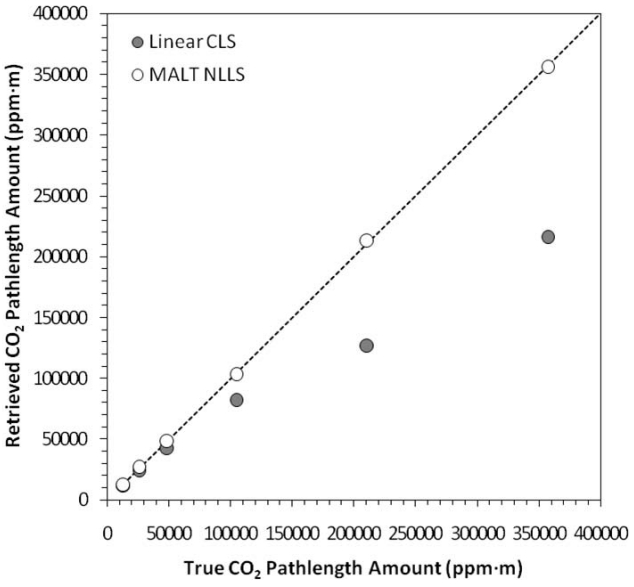

Fig. 1. Comparison of FTIR-derived retrievals of gas-cell CO_2 pathlength amount to the true pathlength amount within the cell. Retrievals were made from the same spectra via two approaches, the Classical Least Squares (CLS) approach described in Haaland (1990) and the MALT forward model and nonlinear least squares (NLLS) fitting procedure described in Griffith (1996) and Griffith et al. (2003). The 1:1 line is shown, and the increasing underestimation of the CLS-based retrievals at higher pathlength amounts is clearly evident.

3 Instrumentation and setup

Our study utilised facilities of the UK's Natural Environment Research Council's Molecular Spectroscopy Facility, part of the Rutherford Appleton Laboratory. A stainless steel gas cell of circular cross section was fitted with IR transparent KBr windows at each end and was filled with the sample gas at the concentration of interest before each spectral measurement. Gas cell length was 1.05 m, diameter 160 mm and IR window diameter 135 mm. The spectrometer used

Table 1. Cell mixing ratios (ppm) and equivalent pathlength amounts (ppmm) for the 1.05 m gas cell filled with CO_2, CH_4 and CO respectively, with the equivalent mixing ratios for longer atmospheric paths (assuming the same temperature, ∼20 °C, and pressure, ∼1000 hPa conditions) also given. For reference, ambient "clean" air mixing ratios of CO_2, CH_4 and CO are circa 385 ppm, 1.8 ppm and 0.15 ppm, respectively.

Cell mixing ratio (ppm)	Cell Pathlength amount (ppmm)	Equivalent mixing ratio for a 30 m path (ppm)	Equivalent mixing ratio for a 100 m path (ppm)	Equivalent mixing ratio for a 800 m path (ppm)
		CO_2		
12 014	12 612	420.4	126.1	15.8
24 991	26 236	874.5	262.4	32.8
45 799	48 080	1602.7	480.8	60.1
100 125	105 112	3503.7	1051.1	131.4
200 200	210 172	7005.7	2101.7	262.7
340 351	357 304	11910.1	3573.0	446.6
		CH_4		
51.94	54.52	1.83	0.55	0.07
92.81	97.43	3.25	0.97	0.12
168.51	176.91	5.90	1.77	0.22
270.85	284.34	9.48	2.84	0.36
490.09	514.50	17.15	5.15	0.64
		CO		
18.96	19.90	0.66	0.20	0.03
244.14	256.30	8.54	2.56	0.32
459.13	482.00	16.07	4.82	0.60
1217.05	1277.67	42.59	12.78	1.60
6077.20	6379.91	212.66	63.80	7.98

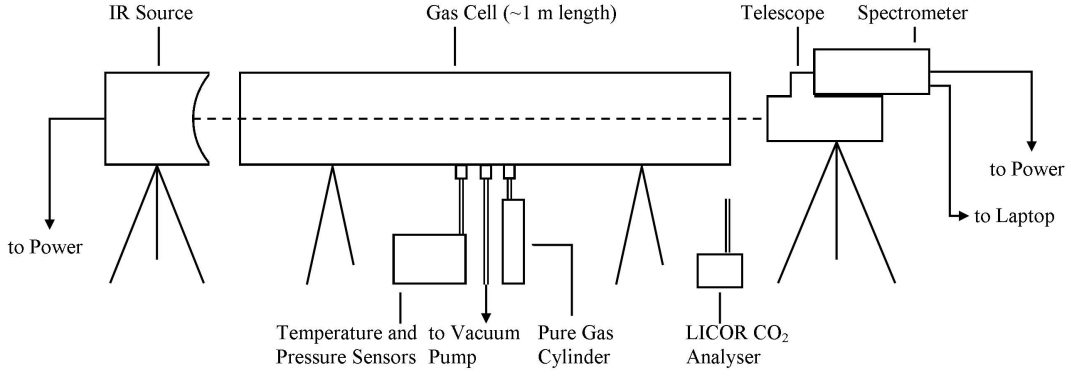

Fig. 2. Schematic of the physical instrumentation arrangement used in the current study.

was a MIDAC Corporation FTIR Air Monitoring system, fitted with a mercury cadmium telluride (MCT) detector and ZnSe optics. The spectrometer was optically coupled to a 76 mm Newtonian telescope and placed to view an IR source through the IR transparent windows of the gas cell. The IR source used was a SiC globar operating at 1100 K, positioned at the focus of a 150 mm collimator. This setup, shown in Fig. 2, is very similar to that used by Horrocks et al. (2001), with a total pathlength of ∼1.5 m, 0.5 m of which consisted of free air between the cell and spectrometer and cell and IR source, together with air inside the spectrometer housing. The CO_2 and H_2O mixing ratios in the ambient air *outside of the cell* were monitored using a calibrated LICOR 840 NDIR gas analyser. An attenuator was fitted to

the FTIR spectrometer telescope to avoid MCT detector saturation, and the temperature of the gas inside the gas cell measured using a platinum resistance thermometer (PRT).

Table 1 lists the gas mixtures investigated. As described by the Beer-Lambert law (Eq. 1), it is possible to simulate a longer OP measurement pathlength by increasing the mixing ratio of the gas sample inside the cell, since pathlength (L) and mixing ratio (c) equivalently increase the number of gas molecules in the open path over which the IR spectra are acquired. However, for target gas mixing ratios above ∼1% (in air or N_2) the linewidths will become significantly affected by self broadening relative to longer path-lower concentration spectra of the same total pathlength amount. This affects each of the CO_2 mixtures used in this study, but not the other gases since their mixing ratios are significantly lower. The MALT model includes a mixing ratio-weighted linewidth to account for this self broadening effect.

The mixing ratios used here were chosen to represent a range covering those from clean air measured over short-to-long pathlengths in the natural environment (e.g. 10–1000 m), as well as polluted air across the same pathlength range, and range up to mixing ratios that might be found in pollutant plumes (e.g. from industrial sources or biomass burning). For example, six different CO_2 pathlength-concentration products (hereafter called pathlength amount) were used, spanning ∼12 500 ppmm to ∼360 000 ppmm. If these pathlength amounts are expressed as mixing ratios using pathlengths typically employed in the field, both the lowest and highest cell mixing ratios yield a CO_2 mixing ratio of ∼420–450 ppm for a 30 m and 800 m path respectively, equivalent to typical ambient CO_2 conditions found in urban settings (e.g. Rigby et al., 2008).

Gas mixtures were prepared manometrically using high purity (99.9%) component gases. The mixing method relied on three MKS Baratron (type 690) pressure capacitance manometers operated at three precision levels of 0.1 Pa, 10 Pa and 100 Pa with a stated accuracy of ±0.05%. The manometers were also used to test the sealing of the gas cell, recording a <1% change in cell pressure over 18 h when filled to ambient pressure (1000 hPa). For each gas concentration to be studied, the cell was evacuated before the sample gas (CO_2, CO or CH_4) was slowly released into the cell until the desired mixing ratio was reached. After waiting for the pressure to stabilise and noting the final pressure, the cell was filled with nitrogen to ambient pressure (1000 hPa) and allowed to stabilise once more. After stabilisation, 10 IR spectrum were measured with the FTIR spectrometer, each consisting of 8 co-added scans (a total of ∼9 s scan time per spectra) in order to increase signal-to-noise. The relative standard deviations among each set of 10 replicate single beam spectral measurements ranged from 0.1–1.2%, with standard errors of the means of 0.03–0.4% for these measurement conditions. The partial pressure of the sample gas was used to calculate the true sample mixing ratio (ppm) by dividing the partial pressure of the sample gas by the final ambient pressure of the gas cell. To avoid contamination by gas from the previous mixture, the lowest concentration of each gas was mixed first, working up to higher concentrations.

4 Procedure for gas concentration retrieval

4.1 Spectrum simulation and fitting algorithm

Spectra were analysed using a NLLS method combined with a forward modelling approach, whereby NLLS was used to fit a modelled spectrum to a measured spectrum, thus solving the inverse problem of returning gas concentrations from the observations. The method is quite commonly applied in OP-FTIR studies, and examples include SFIT2 (Rinsland et al., 1998), often used to retrieve total atmospheric column trace gas abundances (e.g. Hase et al., 2006; Fu et al., 2007 and Senten et al., 2008), but also used for ground-based open-path studies (e.g. Briz et al., 2007). A similar procedure (Burton et al., 1998) has been commonly applied to the retrieval of gas concentrations from open path measurements of volcanic plumes (e.g. Oppenheimer et al., 1998; Horrocks et al., 1999 and Richter et al., 2002). The specific retrieval procedure used here is based on the Multi-Atmospheric Layer Transmission (MALT) model of Griffith (1996) and Griffith et al. (2003), whose past applications include the analysis of open-path, White cell, and solar occultation spectra (Goode et al., 1999; Goode et al., 2000; Bertschi et al., 2003; Galle et al., 2000; Griffith et al., 2002).

The background theory to the inverse problem is detailed in Rodgers (2000). By denoting the measurement spectrum as vector $\boldsymbol{y}$ (the measurement vector) and the variables to be retrieved (the trace gas concentrations) as the state vector $\boldsymbol{x}$, the measurement and its relation to the state vector, can be described as:

$$\boldsymbol{y} = f(x) \tag{3}$$

where $f(x)$ is the forward function, describing the physics of the measurement. It is unlikely that the physics of a system will be known and understood with full accuracy. Hence Eq. (3) is adapted as:

$$y = F(x) + \varepsilon \tag{4}$$

$F(x)$, the forward model, approximates the physics of the measurement, and ε is the measurement error. Here $F(x)$ represents the simulated single beam spectrum.

The radiative transfer forward model used to simulate the spectra $F(x)$ is detailed in Griffith (1996). To parameterise the calculation of $F(x)$ for each measured single-beam spectrum y, the user is required to decide upon an appropriate spectral window for the analysis, and a priori values for component trace gas concentrations, pressure, temperature, pathlength, and instrument line shape. From these, the forward model generates a synthetic single-beam spectrum as a combination of a background spectrum (modelled as a polynomial) and the effect caused by gases having IR absorption

features within the spectral micro-window of interest. Calculations are performed using the HITRAN database (Rothman et al., 2009), listing absorption line positions and strengths, widths and details of pressure and temperature dependencies for the given species.

A polynomial function (the order of which is defined as a parameter by the user) is fitted to the measured spectrum and is used to simulate the 100% continuum line (i.e. the signal in the absence of the trace gas. Examples of different fitted polynomial functions are shown in Fig. 3. The forward model calculates the optical depth (OD) of the target gas at each wavenumber v as a function of the absorption coefficient at v and the pathlength amount of each gas. A necessary parameter for this computation is the Voigt line shape – the convolution of the Doppler broadening Gaussian line shape function and the pressure broadening Lorentzian line shape function. The former is calculated using temperature and molecular weight, and the latter using the pressure dependence given in HITRAN. Convolving the line strengths from HITRAN with the line shape produces the absorption coefficient used to calculate the optical depth. At wavenumber v, the overall OD is taken as the sum of all calculated ODs for all absorption lines for all species. The OD is then converted to a transmission measure and convolved with the instrument line shape (ILS) and the 100% continuum line to yield the final synthetic single-beam spectrum for the spectral window of choice (Fig. 3). The ILS is dependent on the apodization function used, the instrument field-of-view (FOV), and any modulation loss or phase error in the interferometer. These parameters can be retrieved during the NLLS fitting procedure.

The difference between the synthetic and measured spectrum yields a residual spectrum (Fig. 3, bottom); and the chi-squared (χ^2) statistic and the partial derivatives for each of the input parameters are calculated. The Levenburg-Marquardt method (Levenburg, 1944; Marquardt, 1963; Press et al., 1992) is used to find the least-squares linear best fit, and thus the set of optimum gas concentrations that minimise the residual spectrum, based on pre-determined convergence criterion (χ^2 minimum).

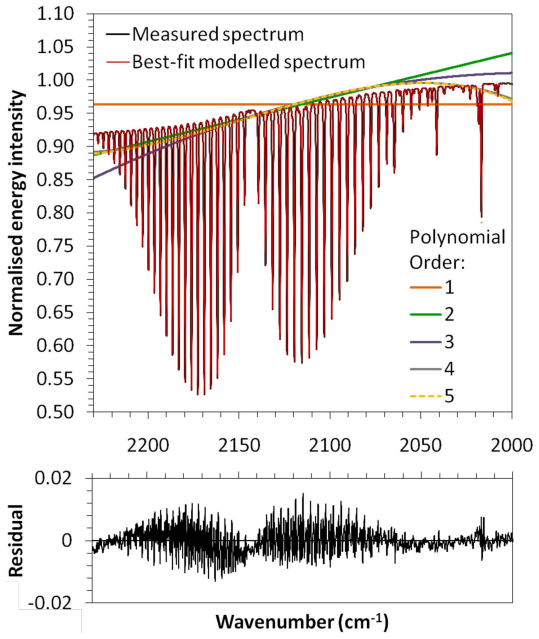

Fig. 3. Examples of results from a measured spectrum and the best-fit modelled spectrum produced using the MALT forward model and nonlinear least squares (NLLS) fitting procedure described in Griffith (1996). The case shown is for 482 ppmm of CO at a gas pressure of 1000 hPa. Top: The measured and best-fit modelled spectra are shown to be well matched, with the different background polynomial functions (orders 1–5) tested also shown. The fourth order polynomial provided the best match to the measured spectrum, and this was used to simulate the best-fit modelled spectrum shown. Bottom: The residual spectrum (i.e. the measured spectrum subtracted from the modelled spectrum), which is used to provide a measure of fitting accuracy. The spectral features in the residual are due to an imperfect fit between the modelled ILS and the non-ideal instrument ILS.

4.2 Reported error

As with other spectrally-based retrieval approaches based on forward modelling and nonlinear fitting methods (e.g. Burton, 1998), MALT reports the standard error for each of the retrieved trace gas amounts and the a priori input parameters (this metric is termed the reported error hereafter). For each iteration of the NLLS fitting procedure, the covariance matrix is determined from the standard deviation of the residual spectrum (i.e. the synthetic spectrum subtracted from the measured spectrum). The reported error for parameter x_i is defined as the square root of the i-th diagonal element of the covariance matrix, and is influenced by choice of a priori fixed input parameters, model errors/lack of fit, measurement noise, amount of information (the width of the spectral window and intensity of signal within that window) and degrees of freedom (which reduces with increasing number of parameters).

The reported error is based on the quality of the fit between the measured and modelled spectra, and is in part designed to provide the user with information potentially useful in gauging the quality of the retrieval process. Most ideally the user would like to know the actual retrieval error, i.e. the true difference between the amount of trace gas present in the optical path and that reported by the retrieval procedure. This retrieval error can have both random and systematic components, and improved understanding of the relationship between the reported error and retrieval error is one of the key aims of this work, along with an appreciation of the absolute accuracies able to be obtained from the method, and their sensitivity to model parameterisation uncertainty.

5 Methodology

5.1 Determination of input parameters

When performing a spectral fit, the input parameters required by the spectral model (MALT) can be stated as fixed constants or can be included in the fitting process. These parameters relate to the composition of the sample atmosphere (i.e. which gases are present in the sample and have absorption lines in the spectral window of interest, the concentration of these gases, and the temperature and pressure of the composition) and to the instrument line shape (i.e. spectral shift, resolution, apodisation, FOV, phase and zero-line offset). In our experiment, whilst the gas concentration was fitted, the temperature and pressure of the sample were taken from the gas cell PRT and Baratron readings respectively. Determination of instrument line shape parameters was, however, less straight forward:

- the spectral shift (correction for fractional wavenumber shifts in the position of absorption lines caused by inaccurate knowledge of the interferometer alignment) was fitted
- the spectral resolution was fixed at the manufacturer's specification ($0.5\,cm^{-1}$)
- asymmetry in the line shape influenced by small changes in spectrometer alignment was also fitted through a variable phase error
- the field-of-view (determined by the spectrometer's limiting aperture and collimator focal length) was initialised at the manufacturer's specification and fitted as described below to determine the effective value.

Horrocks et al. (2001) demonstrate that their MIDAC spectrometer's effective field-of-view of 52 mrad differed significantly from the nominally quoted 20 mrad. We followed the methodology of Horrocks et al. (2001) to determine the field-of-view of the instrument used here, measuring the spectrum of CO gas with narrow absorption lines at low pressure (401 hPa) so that the resulting measurement is primarily a function of the absorption feature convolved with the instrument line shape. 80 scans were co-added to create one particularly low-noise spectrum. A series of MALT retrievals were run for a single absorption line at $2082\,cm^{-1}$, and the field-of-view parameter optimised to give the lowest reported error, whilst all other parameters remained fixed. The FOV parameter yielding the smallest reported error for the low-pressure CO absorption line was used as a fixed input for all other retrievals conducted here. Sensitivity to this parameter was also investigated (see Sect. 5.3).To determine the retrieval error of the reported concentrations, it is necessary to compare the retrieved concentrations with the true concentration (i.e. to the cell concentrations listed in Table 1). Retrieval error is therefore here defined as the true concentration subtracted from the reported concentration, divided by the true concentration and expressed as a percentage.

One further consideration for the retrieval procedure is to account for any zero-baseline spectral offset that may result from photometric errors associated with the use of an MCT detector (Müller et al., 1999). Two factors might lead to a non-zero signal in spectral regions that should otherwise exhibit complete absorption. The first is caused by scattering of radiation that has not originated from the lamp source, potentially related to imperfections in instrument optics, such as dirty mirrors. This is a common occurrence in well used field spectrometers, particularly when deployed to dusty or corrosive environments. Furthermore, if the gas cell was at a different temperature to that of the interferometer, an effect will appear in the measured spectrum. Whilst laboratory spectrometers often solve this problem by placing the interferometer before the sample cell, this is not of the case for bistatic OP-FTIR field configurations (Müller et al., 1999). Neither the temperature of the gas cell nor spectrometer were controlled in this experiment, but were rather left to equilibrate to ambient temperature, and therefore small differences in temperature may have influenced the recorded spectra. The second factor which might lead to a non-zero baseline is detector saturation. MCT detectors saturate rather easily (Smith, 1995), and whilst efforts were made in this study to prevent detector saturation via use of the attenuator, some detector saturation effect may be present. Any zero-baseline offset caused by stray light or detector saturation will be apparent in spectral regions where the examined gases should absorb all incoming radiation (e.g. the CO_2 saturation band at $\sim 2350\,cm^{-1}$). If an offset was present, this amount was subtracted from the spectrum before quantitative analysis.

5.2 Spectral window and "background" polynomial

MALT requires the user to select a suitable spectral window and an appropriate polynomial for simulating the continuum spectra. To yield the most accurate concentrations, the window must have sufficient information about the gas of interest (i.e. an absorption feature) and should ideally be in a region of the IR spectrum that minimises contaminating absorption features from other gases (though this is not essential). The order of the polynomial used to simulate the continuum spectrum needs to be carefully selected so that it does not fit broad absorption features. In this work, a series of spectral windows were tested for retrieving the concentrations of each gas (Fig. 4 and Table 2), and the window yielding the lowest retrieval errors was thus identified. Similarly, a range of polynomial orders (3rd, 4th and 5th order) were employed. Given that all three gases in this study demonstrate fine absorption structure (a number of clearly defined narrow absorption lines) within the tested spectral windows, it is unlikely that the background polynomial fit will be influenced

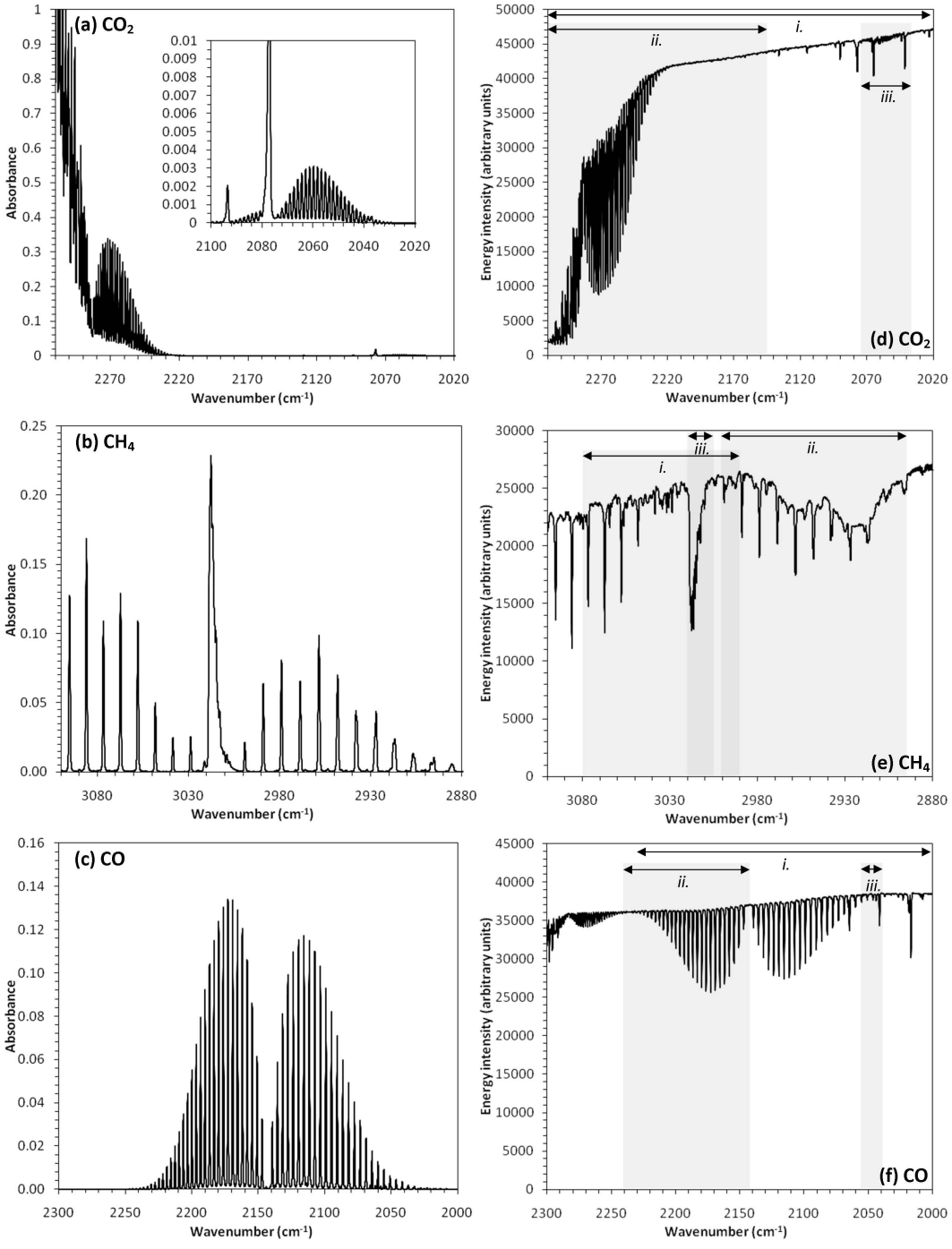

Fig. 4. Modelled and measured spectra at 0.5 cm^{-1} wavenumber resolution for the CO_2, CH_4, and CO trace gases considered here. (left) Absorbance spectra modelled using the MALT forward model; (right) Measured FTIR single-beam spectra. The various spectral windows used to retrieve the trace gas concentrations from the measured spectra are indicated by the numbered horizontal arrows in **(d)**, **(e)**, **(f)** and are detailed in Table 2.

by these, except perhaps across the narrow CH_4 spectral window.

For CO_2 (Fig. 4a and d), the widest spectral spectral window used here, 2020–2310 cm^{-1} (taken from Esler et al., 2000) was split into two sub windows, 2150–2310 cm^{-1} (location of primary absorption features of $^{13}CO_2$ and $^{12}CO_2$) and 2034–2075 cm^{-1} (location of the weaker $^{12}CO_2$ feature, see inset in Fig. 4a). For each window, CO_2 retrievals were run using a background continuum spectrum simulated via 3rd, 4th and 5th order polynomials. Given that water

Table 2. Spectral windows used here for the retrieval of CO_2, CH_4 and CO and marked in Fig. 4. Also listed are the potentially interfering gases (those in brackets were not included in the forward-model spectral simulation conducted here due to the very short clean air atmosphere path used, but would generally be required over longer pathlengths in the ambient atmosphere).

Target Gas	Spectral window	Interfering gases
CO_2	2020–2310 cm^{-1}	H_2O (N_2O, CO)
	2034–2075 cm^{-1}	H_2O
	2150–2310 cm^{-1}	H_2O (N_2O, CO)
CH_4	2894–3001 cm^{-1}	H_2O
	2980–3090 cm^{-1}	H_2O
	3005–3020 cm^{-1}	H_2O
CO	2000–2230 cm^{-1}	H_2O
	2039–2057 cm^{-1}	H_2O
	2142–2241 cm^{-1}	H_2O

vapour was certainly present in the ambient part of the path external to the gas cell and has absorption lines in these spectral windows, H_2O was also included in the retrievals. Whilst CO and N_2O also absorb within these spectral windows, they were not present in sufficient amounts to be significant. In field situations using longer pathlengths, CO and N_2O may affect the measured signal and should therefore be included in any retrieval procedure. For CH_4, Esler et al. (2000) use a broad spectral window, 2810–3150 cm^{-1}. Unfortunately, the majority of this window is affected by a spectrometer artefact (2800–2990 cm^{-1}, see Fig. 4b and e), believed to be caused by residue on the instrument optics. The complexity introduced by the artefact significantly hinders the ability to model the spectrum using a lower-order (<6) polynomial. Two spectral windows were therefore selected so as to exclude the effects of this artefact, a broad window (2980–3090 cm^{-1}), that maximises the number of CH_4 absorption lines, and a narrower window concentrating on the strongest lines (3005–3020 cm^{-1}). In addition, a third window, lying within the region where lines are affected by the detector artefact (2894–3001 cm^{-1}) was also investigated. For CO (Fig. 4c and f), Esler et al. (2000) use a broad window encompassing the entire CO absorption feature and a similar window is used here (2000–2230 cm^{-1}). In addition, two narrower windows, one featuring only one branch of the CO absorption feature (2142–2241 cm^{-1}) and the other featuring only four weaker CO absorption lines (2039–2075 cm^{-1}) were also investigated.

5.3 Sensitivity analysis and error budget

A local sensitivity analysis was performed in order to determine the influence of model parameter uncertainty on retrieval accuracy. Uncertainties in temperature, pressure and spectrometer FOV were considered, which may result from field situations where the measurement conditions are less tightly controlled than is possible in the laboratory. In particular, it can be difficult to measure temperature and pressure precisely in some open-path geometries, particularly when analysing high altitude plumes, or ones where the plume is generated by high temperature volcanological or combustion-related processes. Pressure and temperature are important in the retrieval procedure as they affect the shape of gas absorption features upon which the fit between the measured and modelled spectra depends. Assumed pressure determines the Lorentzian line shape of absorption lines in the simulated spectra. Higher pressures lead to a broadening of line widths, and the maximum line depth is suppressed. Whilst the relatively low (0.5 cm^{-1}) spectral resolution of the FTIR spectrometer used here is responsible for the majority of observed linewidths, this pressure-related broadening does also influence the retrieval process. Pressure broadening for any sample gas is also related to the other gases contained in the gas mixture.

The influence of assumed temperature is to affect the strengths of individual absorption lines and the band shape of the modelled spectra. Doppler broadening caused by the temperature-dependent distribution of molecular velocities within gases (as well as a minor influence on line broadening) contributes to the temperature dependence of lineshapes. The primary influence of temperature and pressure, however, is in the calculation of the mixing ratio from the retrieved number of gas molecules per square cm (molecules cm^{-2}) output from the retrieval process (the absorption features present in the spectra are a direct function of the number of molecules of the target gas in the optical path). The relationship between the concentration of a particular gas in a sample, in molecules per square centimetre (X, molecules cm^{-2}) and the mixing ratio of the gas (x, ppm), pressure (p, hPa), temperature (T, K) and pathlength of the sample (L, m) is described in Eq. (5), where A is Avogadro's constant (6.022×10^{23} mol^{-1}) and R is the gas constant (8.314 J $[mol\ K]^{-1}$):

$$X = \frac{xLpA}{RT} \tag{5}$$

Any error in assumed pressure or temperature will therefore cause a proportional error in retrieved mixing ratio (x) through Eq. (5); whereas, retrievals in molecules cm^{-2} will only be affected by the influence of pressure and temperature errors on the modelled spectra. In many applications, OP-FTIR is used to investigate concentration ratios of two gases, for example CO_2:CO in biomass burning studies (Yokelson et al., 1997) or SO_2:HCl in volcanological applications (Burton et al., 2007), and in this case it may not be necessary to retrieve volumetric mixing ratios since the ratios of the gas amounts expressed in units of molecules cm^{-2} or ppmm is identical. Therefore, for the sensitivity analysis conducted

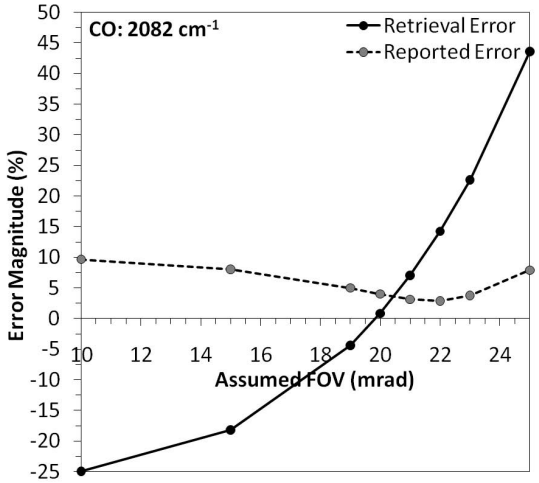

Fig. 5. Sensitivity of the reported error (based on the fit residuals) and retrieval error (based on the difference between retrieved pathlength trace gas amount and actual pathlength trace gas amount) to assumed instrument FOV. The example is shown for CO trace gas retrievals based on the CO absorption line centred at 2082 cm^{-1} (Fig. 6). Measurements were made at a low pressure of 400.5 hPa with a true CO mixing ratio of 1217.05 ppm. Reported error is minimised at an assumed FOV of 22 mrad, though is relatively insensitve to the FOV variations studied here. Retrieval error is, however significantly more sensitive, and assumed 20 mrad FOV yields the smallest actual retrieval error.

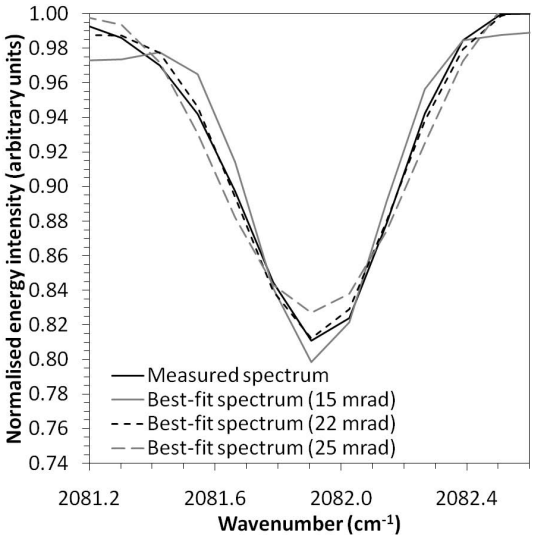

Fig. 6. Measured single-beam spectra and best-fit modelled spectra for the CO absorption line centred at 2082 cm^{-1} at a gas pressure of 400.5 hPa. Modelled spectra were simulated assuming different fields-of-view (15–25 mrad), with the 22 mrad FOV providing the best match between the measured and modelled spectra.

here, pressure and temperature-independent amounts (in molecules cm^{-2}) were used for the comparison. Pressure and temperature inputs were varied systematically by up to $\pm 20\,^{\circ}C$ and ± 200 hPa respectively; ranges that might be found over altitude differences of up to 3 km. Retrieved concentrations were compared with true concentrations to yield both the retrieval error and sensitivity to the pressure and temperature assumptions.

6 Results and discussion

6.1 FOV determination

Figure 5 shows how the reported error (i.e. the MALT fitting error, quantified as a percentage of the retrieved concentration in Sect. 4.2) and the actual retrieval error (quantified as the percentage difference between the retrieved gas concentration and the true gas concentration in Sect. 4.2) varies with assumed field-of-view. Actual retrieval error is much more sensitive to FOV variations than is the reported error. The lowest reported error occurs at a FOV of 22 mrad, whereas the lowest retrieval error occurs at a FOV of 20 mrad. Assumed FOV significantly larger or smaller than the 22 mrad optimum value resulted in increasingly poor fits between the modelled and measured CO spectrum (Fig. 6). Unlike Horrocks et al. (2001), we found the optimal FOV, according to the reported error, to be similar to the nominal FOV stated by the instrument manufacturer, and we attribute the 2 mrad (10%) discrepancy to off-axis rays caused by a combination of small misalignments of spectrometer and telescope optics, and an imperfect source collimator. Horrocks et al. (2001) also found a discrepancy between the FOV parameter yielding the lowest reported error and those that yielded the lowest retrieval error. This discrepancy may be explained by our use of nitrogen as a buffer gas, given that line broadening coefficients in the HITRAN08 database (Rothman et al., 2009) relate to the gas of interest in air, and not when mixed with nitrogen. The difference between nitrogen and air broadening is of the order of $\sim$10%. This factor, combined with uncertainties in HITRAN, or an inability of the forward modelling and NLLS fitting procedure to accurately retrieve concentrations using a single absorption line given the relatively low spectral resolution of the instrument, may also explain this discrepancy. By retrieving concentrations using broader spectral features, the retrieved effect of instrument line shape inaccuracies on individual absorption lines are decreased. The effects of degrading the assumed spectral resolution from the highest 0.5 cm^{-1} value were investigated, but increased the reported errors, and therefore further adjustments to this factor were not required.

6.2 Spectral window and background polynomial

6.2.1 Carbon dioxide

For each gas, three spectral windows were identified containing either a broad absorption feature or a selection of

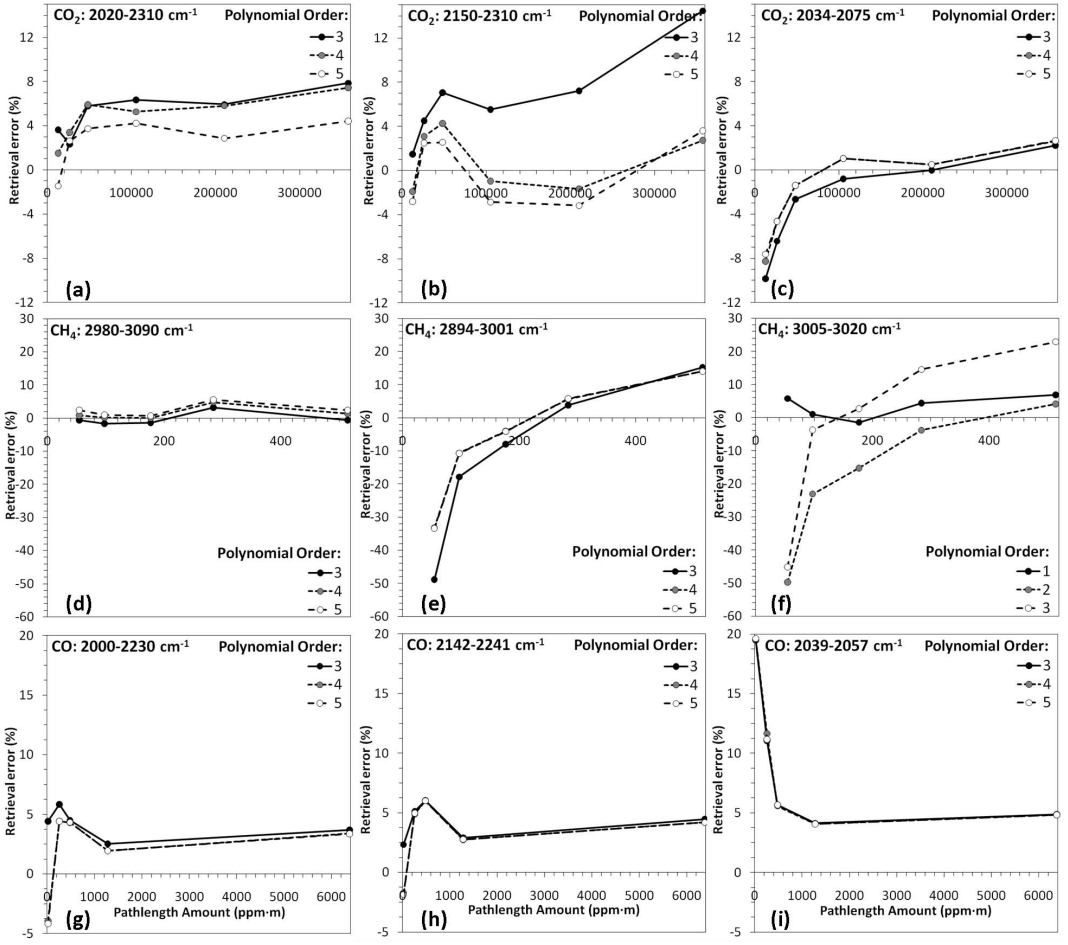

Fig. 7. Retrieval errors for CO_2, CH_4 and CO trace gas retrievals resulting from use of the MALT model and NLLS fitting procedure with OP-FTIR spectra from a gas cell containing samples of these three gases over wide concentration ranges. Retrievals were made using three different spectral windows for each trace gas and three different polynomial orders. In order to aid comparison of the error magnitudes for the retrievals of each trace gas, the same y-axis range is used to display the results from the three spectral windows tested. Retrieval error magnitude is seen to vary quite widely between the different spectral windows used to retrieve the pathlength amount of a particular trace gas, and for some windows between the different polynomial orders examined.

individual absorption lines (Fig. 4 and Table 2). For CO_2, results shown in Fig. 7 indicate that the absolute retrieval error for 5 of the 6 pathlength amounts tested is at a minimum for the 2150-2310 cm^{-1} spectral window using a fourth-order polynomial, with retrieved pathlength amounts over the full range tested having a root mean squared (RMS) error of 2.4% (Fig. 7b). Whilst the results show little sensitivity to the use of a fourth or fifth-order polynomial, the use of a third-order polynomial leads to a noticeable increase in retrieval error. A third-order polynomial is insufficient to describe the background shape of a spectral window as wide as 2150–2310 cm^{-1}. Moreover, the background shape of this window is complicated by the CO_2 absorption feature that strengthens to saturation at 2310 cm^{-1} (Fig. 4a). Retrieval errors are highest for the broader, 2020–2310 cm^{-1} spectral window (Fig. 7a), though the reported error (not shown) is lowest for this window (0.1%, compared with 0.3% for 2150–2310 cm^{-1} and 0.9% for 2034–2075 cm^{-1}). This apparent contradiction may be explained by the presence of a large featureless baseline across most of this wider spectral window (Fig. 4a) leading to an overall improved fit between the modelled and measured spectrum, though not necessarily the best fit at the wavenumber location of the absorption features. A wider spectral window typically decreases the ability of any particular polynomial to model the background continuum as is the case here. There is also an additional reason why use of the broader spectral window generally leads to greater inaccuracy. This is because the zero-baseline offset can only be calculated from data collected in the CO_2 absorption saturation region (near 2350 cm^{-1}), and uncertainties in this correction will increase as the offset is applied to more distant spectral locations. The results for the narrowest

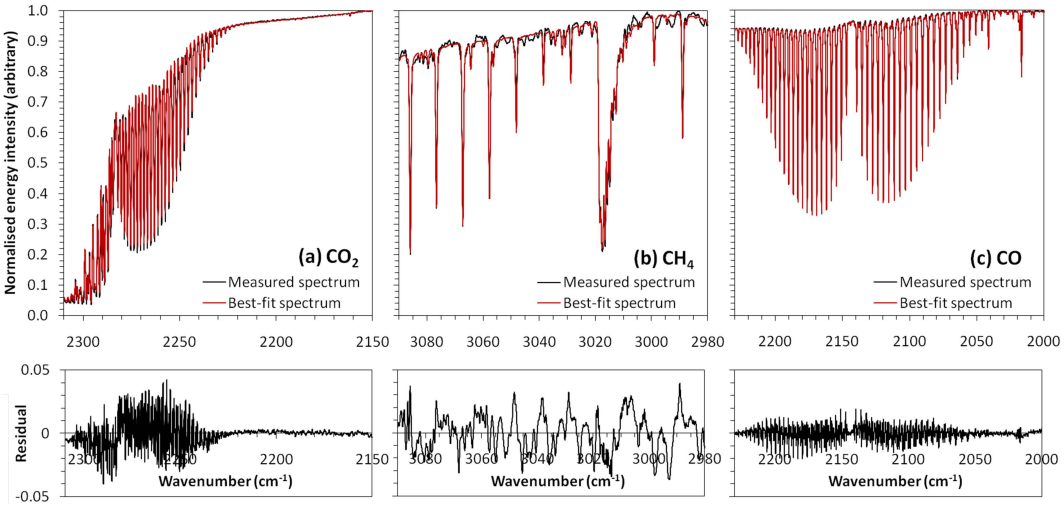

Fig. 8. Examples of measured spectra and best-fit modelled spectra made using the optimum spectral windows and a fourth-order polynomial background (top), and the residual between the measured and modelled spectra (bottom) for **(a)** CO_2; **(b)** CH_4; and **(c)** CO. Modelled spectra were simulated using MALT and the best-fit modelled spectra were found using the NLLS fitting procedure.

spectral window (2034–2075 cm^{-1}) used here for CO_2 retrieval are less influenced by the choice of polynomial order, each having RMS errors of less than 3.7% (Fig. 7c). The flatter background continuum in this window, combined with the presence of fine absorption structure in the CO_2 lines, explains the reduced sensitivity to polynomial order. The inaccuracy of the retrievals made at lower pathlength amounts in this spectral window is most likely due to the weaker nature of the absorption lines at 2034–2075 cm^{-1}.

Our results clearly indicate that the choice of spectral window, coupled with an appropriate choice of background polynomial, have a strong influence on CO_2 retrieval accuracy. Broader windows typically contain more information, potentially improving the fit between the modelled and measured spectra. However, it is also important to ensure that the background continuum of the spectrum within the window under study can be sufficiently well represented by the chosen polynomial. Our results suggest that whilst the 2020–2310 cm^{-1} spectral window used for CO_2 retrieval gives the lowest reported errors (based on the fit residuals; Sect. 4.2), it does not result in the lowest retrieval error. The 2150–2310 cm^{-1} spectral window, used with a fourth-order polynomial actually provides the lowest retrieval error for CO_2, ranging from −1.9% to 4.3% across all pathlength amounts tested. An example spectrum with best-fit modelled spectrum is shown in Fig. 8a.

6.2.2 Methane

As outlined in Sect. 5.2, retrievals of CH_4 were confounded by an instrument artefact in the relevant absorption region. The spectral window tested that covered this region (2894–3001 cm^{-1}) showed both large reported and retrieval errors, regardless of the polynomial order chosen (Fig. 7e). The lowest retrieval errors for CH_4 come instead from the 2980–3090 cm^{-1} spectral window that excludes the artefact region (Fig. 7d), with a fourth-order polynomial yielding an RMS error of 1.4% (Fig. 8b shows an example spectrum with a best-fit modelled spectrum for this spectral window). As was the case with the narrowest (2034–2075 cm^{-1}) CO_2 retrieval window, the polynomial order does not significantly influence retrieval accuracy due to the fine structure of the CH_4 absorption lines and the flat background continuum. However, for the narrowest CH_4 retrieval window tested (3005–3020 cm^{-1}), the polynomial order has a strong influence (Fig. 7f) with only a first order function allowing pathlength amounts to be retrieved within an RMS error of 3.9%. Individual CH_4 absorption lines remain unresolved at the 0.5 cm^{-1} spectral resolution used here, and instead combine to appear as one large apparent absorption feature, and thus higher order polynomials incorrectly start to fit this feature as well as the background continuum.

6.2.3 Carbon monoxide

Results for CO suggest that the two broadest spectral windows provide very similar retrieval accuracies (Fig. 7g and h), with the 2000–2230 cm^{-1} spectral window used with a fourth-order polynomial achieving an RMS error of 3.6% across all pathlength amounts tested here (slightly better than the RMS error of 3.9% for the 2142–2241 cm^{-1} spectral window). Figure 8c shows an example spectrum and best-fit modelled spectrum for the spectral window 2000–2230 cm^{-1}. Generally, the two narrower spectral windows overestimated pathlength amounts compared to the 2000–2230 cm^{-1} window. Retrievals for CO across all spectral

windows tested here showed a lower reliance on choice of background polynomial compared to the other gases, reflecting the "flat" background continuum across the whole CO absorption feature (Fig. 4f). Results from the narrower 2039–2057 cm^{-1} spectral window indicate that it is best suited to retrieval of higher pathlength amounts (Fig. 7i), with poor retrieval accuracies for pathlength amounts below 1000 ppmm. High reported errors (based on the fit residuals) suggest that the retrieval process performs poorly with the weak absorption lines in this spectral window, as is also the case for lower pathlength amounts of CO_2 retrieved in the 2034–2075 cm^{-1} spectral window.

6.3 Sensitivity analysis and error budget

Using the optimum set of retrieval parameters described in Sect. 6.2, a series of sensitivity analyses were performed. In Sect. 6.1, the spectrometer FOV was determined as 22 mrad. The exact FOV is difficult to determine given the fast optics and the absence of a well defined limiting aperture. We compared retrievals made using our optimally determined FOV with those made using a FOV varied by ±10%.

Retrievals for all three gases generally show a systematic reliance upon the specified FOV (Fig. 9), with retrieved pathlength amounts generally increasing with assumed FOV. CO demonstrated the greatest sensitivity to FOV since the CO absorption lines are narrower than the instrument's 0.5 cm^{-1} spectral resolution and their representation is therefore strongly influenced by instrument parameters. CO_2 retrieval accuracy appears to be less sensitive to FOV uncertainty at higher pathlength amounts. This may be explained by the increasing saturation (absorption of all source energy) by strong absorption lines at higher CO_2 pathlength amounts, leaving fewer lines in the spectral window affected by errors in FOV.

The retrieval sensitivities to assumed pressure and temperature were calculated from the pressure- and temperature-independent molecular amounts (molecules cm^{-2}), rather than from the volumetric mixing ratios (ppmm), as the latter are additionally sensitive to these parameters via the relationship used to interconvert between these two concentration units (Eq. 5). Figure 10 shows the sensitivity of the retrievals to assumed gas pressure, where it can be seen that pathlength amounts are generally overestimated when pressure is underestimated, and vice versa. As is the case with the FOV parameter, the modelled absorption line widths are affected by the assumed pressure (Fig. 11a and b). When a lower pressure is assumed, narrower lines than are actually present in the measured spectrum are modelled due to inadequate pressure broadening, causing a positive residual between the modelled spectrum and the measurement (similar to the residual spectrum in Fig. 11b. In order to fit the modelled spectrum to the measured spectrum, the NLLS procedure increases the concentration of the absorber to minimise this positive residual, leading to an overestimation of

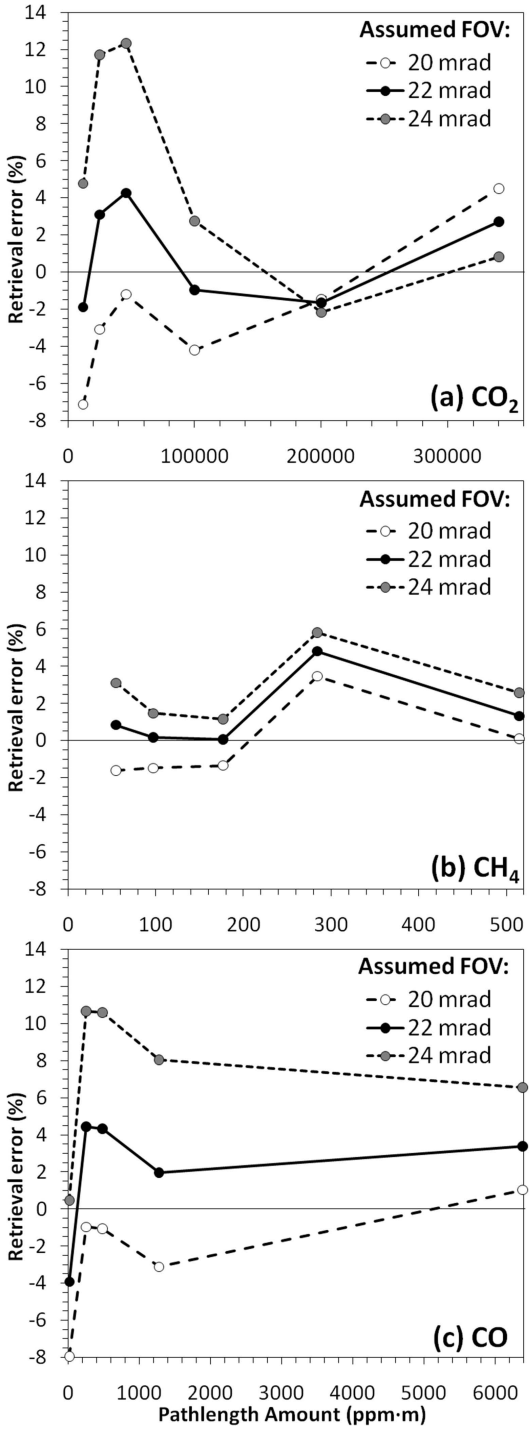

Fig. 9. Sensitivity of trace gas concentration retrieval error to the assumed FOV for **(a)** CO_2, **(b)** CH_4, and **(c)** CO. Retrievals were made using the MALT model with a NLLS fitting procedure. The same y-axis range is used in each case to aid comparison of error magnitude between gases.

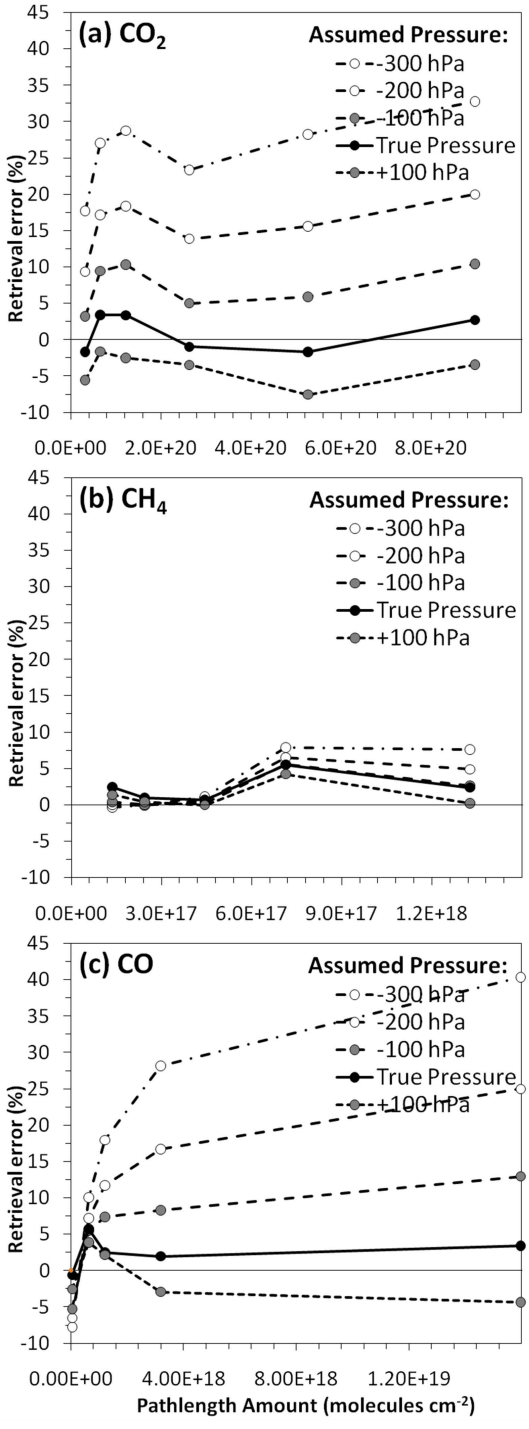

Fig. 10. Sensitivity of trace gas concentration retrieval error to the assumed gas pressure for **(a)** CO_2, **(b)** CH_4, and **(c)** CO. Retrievals were made using the MALT model with a NLLS fitting procedure. The same y-axis range is used in each case to aid comparison of error magnitude between gases.

gas pathlength amounts, whereas the reverse is true when assumed pressure is overestimated.

For CH_4 and lower pathlength amounts of CO, the error induced by pressure uncertainties was significantly lower than for CO_2 (Fig. 10). As pathlength amounts increase, absorption lines deepen, causing any line shape inaccuracies due to incorrect pressure specification to be exacerbated. For CO_2, line deepening is less of an issue, given that deep absorption lines occur for all pathlength amounts in the spectral window chosen, and this explains why CO_2 retrievals shows a higher sensitivity to pressure uncertainties at all pathlength amounts, with the percentage error relatively independent of actual concentration. We find that the reported errors based on the modelled fit residuals show little dependence on pressure ($\pm$0.04%, $\pm$0.01% and $\pm$0.002% across $\pm$100 hPa for CO_2, CH_4 and CO respectively), whereas retrieval errors show a much greater sensitivity. In field situations, pressure uncertainties are most likely to arise from uncertainty in plume height. Our analysis shows that uncertainties of up to 500 m at sea level ($\sim$50 hPa) are therefore equivalent to a $\pm$0.5% uncertainty in CH_4 and low CO pathlength amounts, but are closer to $\pm$3% for CO_2 and higher pathlength amounts of CO.

Figure 12 shows the sensitivity of retrieved pathlength amount to assumed temperature. For CH_4 and CO retrievals, temperature increases lead to proportional increases in retrieved pathlength amounts, whilst for CO_2, this effect is not observed at lower pathlength amounts and is reversed for the highest pathlength amounts (above 5×10^{20} molecules cm^{-2}). These findings are best explained by the temperature dependence of spectral band shape. Changing temperature affects the envelope of the absorption band (Fig. 11c), with higher temperatures causing more absorption in the weaker lines that lie towards the edge of the band, and reduced absorption in the stronger lines located towards the middle of the band. Therefore, for spectral windows containing strong absorption lines located towards the middle of an absorption band, when assumed temperature is overestimated, a higher gas concentration is required for the modelled spectrum to best-fit the measured spectrum. When a spectral window containing weaker absorption lines at the edge of an absorption band is used, the opposite is true. For the CH_4 and CO spectral windows, these effects largely cancel each other out as the spectral windows lie across both strong and weaker lines at the middle and edge of their respective absorption bands. The greater influence of the stronger absorption lines leads to a small positive sensitivity for CH_4 and CO in the spectral windows used here. For CO_2, however, the saturation of the strongest lines towards the middle of the band means that the sensitivity of concentration retrievals to temperature is reversed.

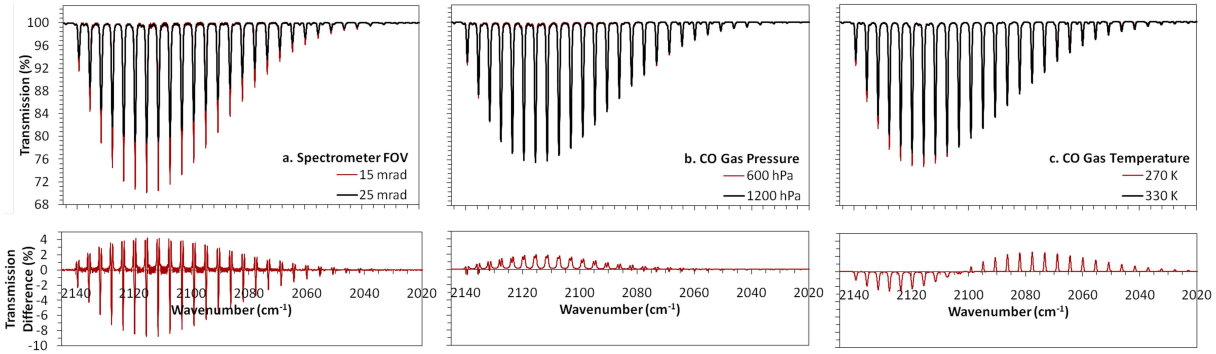

Fig. 11. Simulated transmission spectra for CO gas at a fixed molecular amount of 6.424×10^{17} molecules cm^{-2}, along with percentage difference in transmission between the CO transmission spectra simulated using **(a)** an assumed FOV of 15 mrad and 25 mrad; **(b)** at 600 and 1200 hPa; and **(c)** at 270 K and 330 K. The figure focuses on the *p*-branch of the CO vibrational stretching mode absorption feature, centred at 2143 cm^{-1}. Increasing FOV leads to broader, but weaker absorption lines; increasing pressure leads to deeper and broader absorption lines; whilst increases in temperature lead to stronger absorption towards the edge of the band (wavenumbers < 2100 cm^{-1}) and weaker absorption towards the band centre (wavenumbers > 2100 cm^{-1}).

6.4 Sensitivity summary

Table 3 summarises the findings of the sensitivity analyses and indicates to what percentage accuracy CO_2, CH_4 and CO can be retrieved assuming optimum parameterisation of the forward model. The "worst-case" scenario (as suggested by Horrocks et al., 2001) indicates that the total error due to uncertainties that could arise from incorrect retrieval parameterisation amounts to less than 8.2% for all tested pathlength amounts, with a mean of 4.8%. Generally these "external" errors are of a similar magnitude to the additional errors that maybe introduced via the uncertainty inherent in the absorption line intensities for each gas. The HITRAN08 absorption line intensity uncertainties are reported to be between 5–10% for CO_2 and CH_4, but are lower for CO at 1–2% (Rothman et al., 2009). Of course, with good meteorological measurements and careful collection of non-saturated single-beam spectra, the magnitude of the external errors can be minimised. Whilst a global/variance-based sensitivity analysis may theoretically offer the potential to provide further information about the effects of simultaneous uncertainties in multiple inputs (e.g. Petropoulos et al., 2009), the linear sensitivity of the output gas amounts to uncertainties in the three input parameters suggests that the local sensitivity analysis performed here is perfectly adequate for our purposes.

Errors in assumed pressure become increasingly significant at higher pathlength amounts, due to the deepening of absorption lines, especially for CO_2 and CO. One solution to this problem would be to use a spectral window with weaker absorption lines; however, the results for temperature sensitivities indicate that this would increase sensitivity to the spectral band shape dependence on temperature. Errors in assumed temperature of less than 10 °C lead to errors in retrieved concentration of below 3%. Greater errors are perhaps most likely to occur during studies focused on plumes from hot sources (volcanic, fire or industrial), and care should be taken to minimise sensitivity to these errors by using a broad spectral window encompassing weak and strong absorption lines and ideally targeting plumes once they have cooled to near ambient temperatures at some distance from the source region.

In our experiment, the spectrometer FOV was determined to be 10% higher than the manufacturer's nominal value of 20 mrad. Unlike gases such as SO_2, ambient and elevated pathlength amounts of CO_2, CH_4 and CO demonstrate deep absorption lines that increase their sensitivity to instrument line shape, and therefore extra care should be taken to preserve instrument optics from degradation if measurements are to target these gases.

7 Summary and implications for field measurements

We investigated the accuracy of trace gas retrievals made using a field-portable FTIR spectrometer under conditions that replicated those likely to be encountered in many field situations, e.g. uncertain gas temperature, pressure and instrument line shape/FOV characteristics, and attempted to determine the optimum spectral window within which the retrieval should be made under different measurement conditions. Our study was based on the measurement of gases contained within a 1 m gas cell, from which we collected 0.5 cm^{-1} wavenumber resolution single-beam IR spectra of CO_2, CH_4 and CO over a very broad range of pathlength amounts, representing equivalent mixing ratios from those found in the clean, ambient atmosphere to the highly polluted plumes of biomass burning, volcanoes and industry over pathlengths of tens to hundreds of metres (Table 1).

We used a modelling nonlinear least squares fitting approach to retrieve the concentration of each target gas species. A number of spectral windows were investigated,

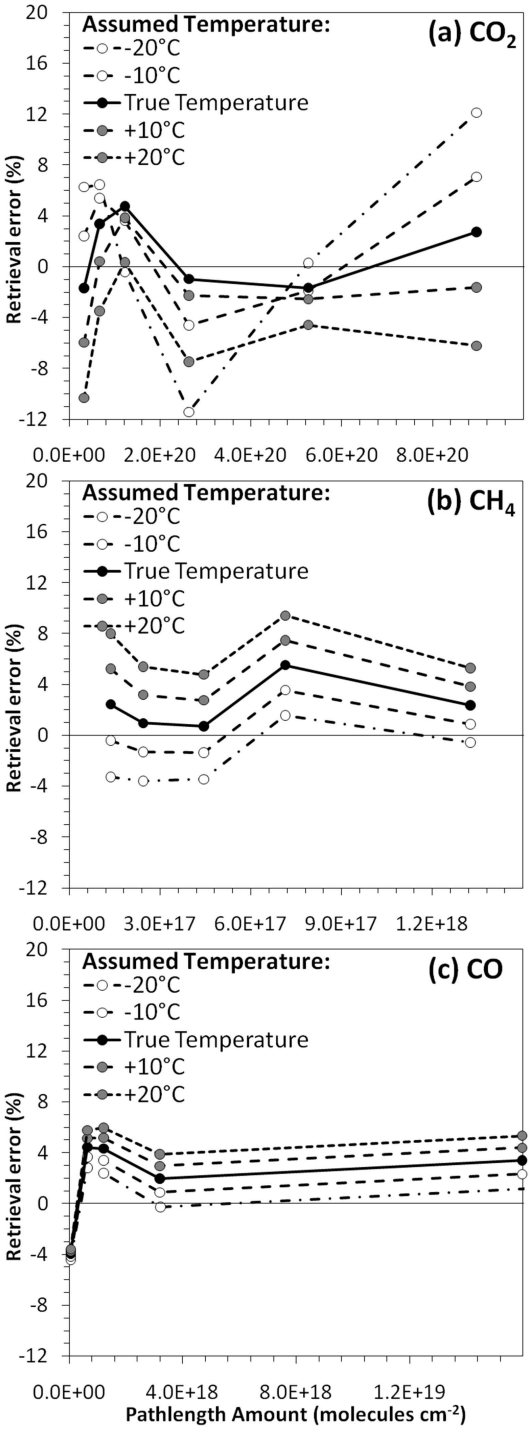

Fig. 12. Sensitivity of trace gas concentration retrieval error to the assumed gas temperature for **(a)** CO_2, **(b)** CH_4, and **(c)** CO. Retrievals were made using the MALT model with a NLLS fitting procedure. The same y-axis range is used in each case to aid comparison of error magnitude between gases.

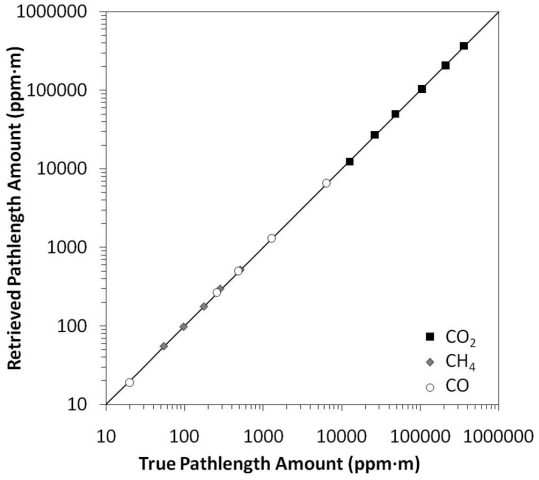

Fig. 13. Relationship between mean retrieved pathlength trace gas amounts made using the optimum parameterisation of the MALT model determined herein. The 1:1 line is shown and all retrieved amounts are within 4.8% of true amounts (note logarithmic axes).

and those that maximised the amount of absorption information for each gas (e.g. the number of absorption lines) typically produced the lowest reported errors (model fit residuals) and the lowest actual retrieval errors when compared to the true gas cell pathlength amount. However, if broad spectral windows are to be used it is important to ensure a good background polynomial fit in the model (which is used to represent the continuum radiation), and we found that when wider windows were investigated, containing large regions showing no absorption (e.g. 2020–2310 cm^{-1} for CO_2), retrieval accuracies were degraded due to poor background fitting. Similarly, it is important to check that broader windows do not contain spectral artefacts, such as those found here in the 2894–3001 cm^{-1} spectral window when retrieving CH_4. Such artefacts, potentially caused by contaminating substances on the spectrometer optics, will complicate the simulation of the continuum background shape using lower-order polynomials, and should be carefully avoided.

When using the optimum parameterisation of the MALT forward model and nonlinear least squares fitting procedure deployed in the retrievals made here, we were able to retrieve trace gas pathlength amounts to within 4.8% of the true values for all gases and pathlength amounts tested (Fig. 13). Mean retrieval errors were 2.4%, 1.4% and 3.6% for CO_2, CH_4 and CO, respectively. A series of analyses was performed to assess the sensitivity of these retrievals to uncertainties in instrument (i.e. FOV) and environmental (i.e. temperature, pressure) parameters. The uncertainties assumed were of a magnitude similar to those expected in the types of field situations in which OP-FTIR may be employed. Sensitivities were shown to vary between target gases. Uncertainty in the FOV had most impact on CO retrieval. This is because the shape of the modelled CO absorption feature is highly

Table 3. Summary of errors associated with parameter uncertainty when retrieving trace gas amounts from OP-FTIR measurements using the MALT foward model of Griffith (1996) with a NLLS fitting procedure. Errors for choice of polynomial and errors in assumed field-of-view, pressure and temperature are taken from the results presented in Figs. 7, 9, 10 and 11, and are calculated using the difference between the retrievals made using the best parameter to those using the altered parameter, expressed as a percentage. For example, at an actual CO_2 pathlength amount of 12 612 ppmm, the retrieved CO_2 column amount based on the retrieval method parameterised with the optimum parameter values was underestimated by just under 2%. Uncertainties in the HITRAN08 database (Rothman et al., 2009) refer to the line intensity error specified therein.

	Retrieval Error (%), for CO_2 pathlength amounts (ppmm):					
Source of Error	12 612	26 235	48 080	105 112	210 172	357 304
Choice of polynomial (4th or 5th order)	0.9	0.6	1.7	1.8	1.5	0.9
Field-of-view (best-fit or manufacturer's)	5.2	6.2	5.5	3.2	0.2	1.8
50 hPa error in assumed pressure	2.2	2.8	3.2	2.1	3.4	3.5
10 °C error in assumed temperature	4.2	4.5	1.0	2.5	0.6	4.3
Total (added in quadrature)	7.1	8.2	6.7	4.9	3.8	5.9
Uncertainty in line intensities (HITRAN08)	5.0–10.0	5.0–10.0	5.0–10.0	5.0–10.0	5.0–10.0	5.0–10.0
Mean reported error	0.2	0.3	0.4	0.4	0.3	0.3
Optimum retrieval model parameters	−1.9	3.1	4.3	−1.0	−1.7	2.7
	Retrieval Error (%), for CH_4 pathlength amounts (ppmm):					
	54.5	97.4	176.9	284.3	514.5	
Choice of polynomial (4th or 5th order)	1.6	0.8	0.6	0.7	1.0	
Field-of-view (best-fit or manufacturer's)	2.4	1.6	1.4	1.3	1.2	
50 hPa error in assumed pressure	0.8	0.4	0.3	0.3	0.6	
10 °C error in assumed temperature	2.8	2.2	2.1	1.9	1.5	
Total (added in quadrature)	4.1	2.9	2.6	2.4	2.2	
Uncertainty in line intensities (HITRAN08)	5.0–10.0	5.0–10.0	5.0–10.0	5.0–10.0	5.0–10.0	
Mean reported error	2.0	0.9	0.6	0.6	0.8	
Optimum retrieval model parameters	0.8	0.2	0.1	4.8	1.3	
	Retrieval Error (%), for CO pathlength amounts (ppmm):					
	19.9	256.3	482.0	1,277.7	6,379.9	
Choice of polynomial (4th or 5th order)	0.2	0.0	0.0	0.0	0.0	
Field-of-view (best-fit or manufacturer's)	4.0	5.4	5.4	5.1	2.4	
50 hPa error in assumed pressure	1.7	0.5	1.3	2.8	4.3	
10 °C error in assumed temperature	0.2	0.8	0.9	1.0	1.0	
Total (added in quadrature)	4.4	5.5	5.6	5.9	5.0	
Uncertainty in line intensities (HITRAN08)	1.0–2.0	1.0–2.0	1.0–2.0	1.0–2.0	1.0–2.0	
Mean reported error	0.5	0.1	0.1	0.1	0.1	
Optimum retrieval model parameters	−4.0	4.4	4.3	2.0	3.4	

dependent on the assumed instrument FOV, due to the particular narrowness of the CO absorption lines which remain unresolved at the 0.5 cm^{-1} resolution used here. The sensitivity of all retrievals to FOV increased when the spectral window used for the analysis contained strong absorption lines, which occurred at higher pathlength amounts for the CH_4 and CO spectral windows, but at lower pathlength amounts for the CO_2 spectral window (where higher pathlength amounts led to absorption saturation, and therefore, a smaller number of observed absorption lines).

Generally, our results indicate that reported errors, which are based on the residuals between the best-fit forward modelled spectra and the measured spectra, are smaller than the actual retrieval errors and do not always vary in the same manner (Table 3). Reported errors should therefore not be regarded as a proxy for actual retrieval error. Reported errors appear most useful for the optimisation of instrument line shape, where minimising the reported error via adjustment of the assumed FOV can improve actual retrieval errors. However, errors in assumed FOV, temperature and pressure can all impart similar effects on the spectral fitting. For example, minimising reported errors by adjusting the assumed pressure could improve the spectral fit, but the same degree of improvement might be achieved by adjusting the FOV, potentially resulting in a quantitatively different retrieved pathlength trace gas amount. These sensitivities and uncertainties suggest that proper assessment of gas temperature, pressure and instrument FOV are important for accurate trace gas

concentration retrieval, given that errors induced by one parameter may be compensated for by adjusting the value of another parameter to minimise reported error, but that this may result in an incorrect retrieval.

We found that retrieval sensitivity to uncertainties in temperature and pressure were relatively small for the magnitude of parameter uncertainty that might be expected in typical field situations. Assuming a potentially "worst-case" scenario of a 50 hPa and 10 °C error in assumed pressure and temperature, and the 10% difference in FOV found here as compared to the instrument manufacturer's specification, pathlength amount retrievals might vary by up to 8.2% (errors added in quadrature). As discussed by Horrocks et al. (2001), gases that demonstrate individual absorption lines that are resolved in the spectra (as opposed to gases such as SO_2, which has broad bands for which individual rotational lines cannot be resolved), are more susceptible to parameter errors affecting spectral line shape. Minimising uncertainty in these parameters is therefore paramount for retrievals of CO_2, CH_4 and CO via a combination of accurate temperature and pressure information, and careful examination of the spectral fit. In particular, as demonstrated in this study, errors due to poor zero-baseline offset correction, incorrect pressure, temperature, and instrument line shape assumptions will all cause a poor fit when a retrieval is performed using a window containing both weak and strong absorption lines, and minimising reported errors in such a window will improve retrieval accuracy.

Our results confirm that a forward modelling approach coupled with a nonlinear least squares fitting routine can be a viable and accurate method for retrieving gas concentrations from OP-FTIR data, in this case using an MCT detector covering a wide spectral range (600–6000 cm^{-1}). Whilst it remains difficult to use the reported errors (model fit residuals) to provide a quantitative measure of actual concentration retrieval error, our results provide confidence that carefully undertaken retrievals made using the forward modelling NLLS method deployed here can indeed provide good retrieval accuracies in the types of field situation where OP-FTIR could be very usefully deployed. Using an optimum parameterisation of the model, we were able to retrieve the concentrations of the three most abundant carbonaceous gases in the atmosphere to better than 5% over a very wide range of pathlength amounts (Fig. 13).

Acknowledgements. We would like to thank NERC MSF and their staff at RAL, particularly Robert McPheat and Kevin Smith, for their invaluable contribution to the experimental component of this work, and Christopher MacLellan and Alasdair MacArthur of NERC FSF for their wide ranging support, including loan of the FTIR spectrometer used here. We are very grateful for the expertise provided by Peter Zemek and Don Mullally (MIDAC Corporation), Clive Oppenheimer (University of Cambridge) and Mike Burton (Istituto Nazionale di Geofisica e Vulcanologia) at various points during the study, including during parts of the measurement campaign. Funding for the studentship of T. E. L. Smith comes from NERC/ESRC Studentship ES/F012551/1. The contribution of Martin Wooster was supported by the NERC National Center for Earth Observation (NCEO).

Edited by: D. Feist

References

Bacsik, Z., Mink, J., and Keresztury, G.: FTIR spectroscopy of the atmosphere I. Principles and methods, Appl. Spectrosc. Rev., 39, 295–363, 2004.

Bertschi, I., Yokelson, R. J., Ward, D. E., Babbitt, R. E., Susott, R. A., Goode, J. G., and Min Hao, W.: Trace gas and particle emissions from fires in large diameter and belowground biomass fuels, J. Geophys. Res., 108(D13), 8472, doi:10.1029/2002JD002100, 2003.

Briz, S., de Castro, A. J., Díez, S., López, F., and Schafer, K.: Remote sensing by open-path FTIR spectroscopy, Comparison of different analysis techniques applied to ozone and carbon monoxide detection, J. Quant. Spectrosc. Ra., 103, 314–330, 2007.

Burton, M. R.: Remote sensing of the atmosphere using Fourier transform spectroscopy, PhD thesis, Department of Chemistry, University of Cambridge, 1998.

Burton, M. R., Allard, P., Mure, F., and La Spina, A.: Magmatic gas composition reveals the source depth of slug-driven strombolian explosive activity, Science, 317, 227–230, 2007.

Childers, J. W., Thompson Jr., E. L., Harris, D. B., Kirchgessner, D. A., Clayton, M., Natschke, D. F., and Phillips, W. J.: Multi-pollutant concentration measurements around a concentrated swine production facility using open-path FTIR spectrometry, Atmos. Environ., 35, 1923–1936, 2001.

Childers, J. W., Phillips, W. J., Thompson Jr., E. L., Harris, D. B., Kirchgessner, D. A., Natschke, D. F., and Clayton, M.: Comparison of an Innovative Nonlinear Algorithm to Classical Least-Squares for Analyzing Open-Path Fourier Transform Infrared Spectra Collected at a Concentrated Swine Production Facility, Appl. Spectrosc., 56(3), 325–336, 2002.

Esler, M. B., Griffith, D. W. T., Wilston, S. R., and Steele, L. P.: Precision trace gas analysis by FT-IR spectroscopy 1. Simultaneous analysis of CO_2, CH_4, N_2O and CO in air, Anal. Chem., 72(1), 206–215, 2000.

Fu, D., Walker, K. A., Sung, K., Boone, C. D., Soucy, M.-A., and Bernath, P. F.: The portable atmospheric research interferometric spectrometer for the infrared, PARIS-IR, J. Quant. Spectrosc. Ra., 103, 362–370, 2007.

Galle, B., Bergquist, B., Ferm, M., Törnquist, K., Griffith, D. W. T., Jensen, N. O., and Hansen, F.: Measurement of ammonia emissions from spreading of manure using gradient FTIR techniques, Atmos. Environ., 34, 4907–4915, 2000.

Gerlach, T. M., McGee, K. A., Sutton, A. J., and Elias, T.: Rates of volcanic CO_2 degassing from airborne determinations of SO_2 emission rates and plume CO_2/SO_2: Test study at Pu'u "O"o cone, Kilauea volcano, Hawaii, Geophys. Res. Lett., 25, 2675–2678, 1998.

Goode, J. G., Yokelson, R. J., Susott, R. A., and Ward, D. E.: Trace gas emissions from laboratory biomass fires measured by open-path Fourier transform infrared spectroscopy: Fires in grass and surface fuels, J. Geophys. Res.-Atmos., 104(D17), 21237–21245, 1999.

Goode, J. G., Yokelson, R. J., Ward, D. E., Susott, R. A., Babbitt, R. E., Davies, A., and Min Hao, W.: Measurements of excess O_3, CO_2, CO, CH_4, C_2H_4, C_2H_2, HCN, NO, NH_3, NCOOH, CH_3COOH, HCHO and CH_3OH in 1997 Alaskan biomass burning plumes by airborne Fourier transform infrared spectroscopy (AFTIR), J. Geophys. Res.-Atmos., 105(D17), 22147–22166, 2000.

Griffith, D. W. T.: Synthetic calibration and quantitative analysis of gas-phase FTIR spectra, Appl. Spectrosc., 50, 59–70, 1996.

Griffith, D. W. T., Mankin, W. G., Coffey, M. T., Ward, D. E., and Riebau, A.: FTIR Remote Sensing of Biomass Burning Emissions of CO_2, CO, CH_4, CH_2O, NO, NO_2, NH_3, and N_2O, in: Global Biomass Burning, edited by: Levine, J. S., The MIT Press, Cambridge, Massachusetts, 230–239, 1991.

Griffith, D. W. T., Leuning, R., Denmead, O. T., and Jamie, I. M.: Air-land exchanges of CO_2, CH_4 and N_2O measured by FTIR spectrometry and micrometeorological techniques, Atmos. Environ., 36, 1833–1842, 2002.

Griffith, D. W. T., Esler, M. B., Paul Steele, L., and Reisinger, A.: Non-linear least squares: high precision quantitative analysis of gas phase FTIR spectra, paper presented at 2nd Intl. Conference on Advanced Vibrational Spectroscopy, Nottingham, 2003.

Grutter, M.: Multi-Gas analysis of ambient air using FTIR spectroscopy over Mexico City, Atmosféra, 16, 1–13, 2003.

Grutter, M., Flores, E., Basaldud, R., and Ruiz-Suárez, L. G.: Open-path FTIR spectroscopic studies of the trace gases over Mexico City, Atmos. Ocean. Opt., 16(3), 232–236, 2003.

Haaland, D. M.: Multivariate calibration methods applied to quantitative FT-IR analyses, in: Practical Fourier Transform Infrared Spectroscopy, Industrial and Laboratory Chemical Analysis, edited by: Ferraro, J. R. and Krishnan, K., Academic, San Diego, 395–468, 1990.

Hart, B. K., Berry, R. J., and Griffiths, P. R.: Effects of resolution, spectral window, and background on multivariate calibrations used for open-path Fourier transform infrared spectrometry, Field Anal. Chem. Tech., 3(2), 117–130, 1999.

Hase, F., Demoulin, P., Sauval, A. J., Toon, G. C., Bernath, P. F., Goldman, A., Hannigan, J. W., and Rinsland, C. P.: An empirical line-by-line model for the infrared solar transmittance spectrum from 700 to 5000 cm^{-1}, J. Quant. Spectrosc. Ra., 102, 450–463, 2006.

Hong, D. W., Heo, G. S., Han, J. S., and Cho, S. Y.: Application of the open path FTIR with COL1SB to measurements of ozone and VOCs in the urban area, Atmos. Environ., 38, 5567–5576, 2004.

Horrocks, L. A., Burton, M. R., and Francis, P.: Stable gas plume composition measured by OP-FTIR spectroscopy at Masaya Volcano, Nicaragua, 1998–1999, Geophys. Res. Lett., 26(23), 3497–3500, 1999.

Horrocks, L. A., Oppenheimer, C., Burton, M. R., and Duffell, H. J.: Open-path Fourier transform infrared spectroscopy of SO_2: An empirical error budget analysis, with implications for volcano monitoring, J. Geophys. Res., 106(D21), 27647–27659, 2001.

Lamp, T., Radmacher, M., Weber, K., Gärtner, A., Nitz, R., and Bröker, G.: Calibration of an Open-Path FTIR spectrometer for methane, ethylene and carbon monoxide using a fixed 20 m multi pass cell, Proc. SPIE, 3107, 126–136, 1997.

Levenburg, K.: A method for the solution of certain non-linear problems in least squares, Quart. Appl. Math., 2, 164–168, 1944.

Marquardt, D.: An algorithm for least-squares estimation of nonlinear parameters, SIAM J. Appl. Math., 11, 431–441, doi:10.1137/0111030, 1963.

Muller, U., Kurte, R., and Heise, H. M.: Investigation of photometric errors in FTIR-spectra obtained in open-path monitoring, J. Mol. Struct., 482–483, 539–544, 1999.

Oppenheimer, C., Francis, P., Burton, M. R., Madejewsky, A. J. H., and Boardman, L.: Remote measurement of volcanic gases by Fourier transform infrared spectroscopy, Appl. Phys. B. Lasers Opt., 67, 505–516, 1998.

Oppenheimer, C., Burton, M. R., Durieux, J., and Pyle, D. M.: Open-path Fourier transform spectroscopy of gas emissions from Oldoinyo Lengai volcano, Tanzania, Opt. Laser Eng., 37, 203–214, 2002.

Petropoulos, G., Wooster, M. J., Carlson, T. N., Kennedy, M. C., and Scholze, M.: A global Bayesian sensitivity analysis of the 1d SimSphere soil-vegetation-atmospheric transfer (SVAT) model using Gaussian model emulation, Ecol. Model., 220(19), 2427–2440, doi:10.1016/j.ecolmodel.2009.06.006, 2009.

Press, W. H., Teukolsky, S. A., Vetterling, W. T., and Flannery, B. P.: Numerical Recipes, Cambridge University Press, Cambridge, 1992.

Richter, D., Erdelyi, M., Curl, R. F., Tittel, F. K., Oppenheimer, C., Duffell, H. J., and Burton, M.: Field measurements of volcanic gases using tunable diode laser based mid-infrared and Fourier transform infrared spectrometers, Opt. Laser. Eng., 37, 171–186, 2002.

Rigby, M., Toumi, R., Fisher, R., Lowry, D., and Nisbey, E. G.: First continuous measurements of CO_2 mixing ratio in central London using a compact diffusion probe, Atmos. Environ., 42, 8943–8953, 2008.

Rinsland, C. P., Nicholas, B. J., Connor, B. J., Logan, J. A., Pougatchev, N. S., Goldman, A., Murcray, F. J., Stephen, T. M., Pine, A. S., Zander, R., Mahieu, E., and Demoulin, P.: Northern and southern hemisphere ground-based infrared spectroscopic measurements of tropospheric carbon monoxide and ethane, J. Geophy. Res., 103(D21), 28197–28218, doi:10.1029/98JD02515, 1998.

Rodgers, C. D.: Inverse Methods for Atmospheric Sounding: Theory and Practice, World Scientific Publishing Co. Ltd., Singapore, 2000.

Rothman, L. S., Gordon, I. E., Barbe, A., Chris Benner, D., Bernath, P. F., Birk, M., Boudon, V., Brown, L. R., Campargue, A., Champion, J.-P., Chance, K., Coudert, L. H., Dana, V., Devi, V. M., Fally, S., Flaud, J.-M., Gamache, R. R., Goldman, A., Jacquemart, D., Kleiner, I., Lacome, N., Lafferty, W. J., Mandin, J.-Y., Massie, S. T., Mikhailenko, S. N., Miller, C. E., Moazzen-Ahmadi, N., Naumenko, O. V., Nikitin, A. V., Orphal, J., Perevalov, V. I., Perrin, A., Predoi-Cross, A., Rinsland, C. P., Rotger, M., Šimeèková, M., Smith, M. A. H., Sung, K., Tashkun, S. A., Tennyson, J., Toth, R. A., Vandaele, A. C., and Vander Auwera, J.: The *HITRAN* 2008 molecular spectroscopic database, J. Quant. Spectrosc. Ra., 110, 533–572, 2009.

Schafer, K., Haus, R., Heland, J., and Haak, A.: Measurements of atmospheric trace gases by emission and absorption-spectroscopy with FTIR, Phys. Chem. Chem. Phys., 99(3), 405–411, 1995.

Schafer, K., Jahn, C., Sturm, P., Lechner, B., and Bacher, M.: Aircraft emission measurements by remote sensing methodologies at airports, Atmos. Environ., 37, 5261–5271, 2003.

Senten, C., De Mazière, M., Dils, B., Hermans, C., Kruglanski, M., Neefs, E., Scolas, F., Vandaele, A. C., Vanhaelewyn, G., Vigouroux, C., Carleer, M., Coheur, P. F., Fally, S., Barret, B., Baray, J. L., Delmas, R., Leveau, J., Metzger, J. M., Mahieu, E., Boone, C., Walker, K. A., Bernath, P. F., and Strong, K.: Technical Note: New ground-based FTIR measurements at Ile de La Réunion: observations, error analysis, and comparisons with independent data, Atmos. Chem. Phys., 8, 3483–3508, doi:10.5194/acp-8-3483-2008, 2008.

Smith, B. C.: Fundamentals of Fourier Transform Infrared Spectroscopy, CRC Press, New York, 224 pp., 1995.

von Bobrutzki, K., Braban, C. F., Famulari, D., Jones, S. K., Blackall, T., Smith, T. E. L., Blom, M., Coe, H., Gallagher, M., Ghalaieny, M., McGillen, M. R., Percival, C. J., Whitehead, J. D., Ellis, R., Murphy, J., Mohacsi, A., Pogany, A., Junninen, H., Rantanen, S., Sutton, M. A., and Nemitz, E.: Field inter-comparison of eleven atmospheric ammonia measurement techniques, Atmos. Meas. Tech., 3, 91–112, doi:10.5194/amt-3-91-2010, 2010.

Yokelson, R. J., Susott, R., Ward, D. E., Reardon, J., and Griffith, D. W. T.: Emissions from smoldering combustion of biomass measured by open-path Fourier transform infrared spectroscopy, J. Geophys. Res., 102, 18865–18877, 1997.

Zhu, C. and Griffiths, P. R.: Extending the range of Beer's law in FT-IR spectrometry, Part I: Theoretical study of Norton-Beer apodization functions, Appl. Spectrosc., 52(11), 1403–1408, 1998.